

Optimal homotopy perturbation method for nonlinear differential equations governing MHD Jeffery-Hamel flow with heat transfer problem

Vasile Marinca^a, Remus-Daniel Ene^{b,*}

^a*University Politehnica Timișoara, Department of Mechanics and Vibration, Timișoara, 300222, Romania*

Department of Electromechanics and Vibration, Center for Advanced and Fundamental Technical Research, Romania Academy, Timișoara, 300223, Romania

^b*University Politehnica Timișoara, Department of Mathematics, Timișoara, 300006, Romania*

Abstract

In this paper, Optimal Homotopy Perturbation Method (OHPM) is employed to determine an analytic approximate solutions for nonlinear MHD Jeffery-Hamel flow and heat transfer problem. The Navier-Stokes equations, taking into account Maxwell's electromagnetism and heat transfer lead to two nonlinear ordinary differential equations. The obtained results by means of OHPM show a very good agreement in comparison with the numerical results and with Homotopy Perturbation Method (HPM).

Keywords: optimal homotopy perturbation method, Jeffery-Hamel, nonlinear ordinary differential equations.

1. Introduction

The incompressible fluid flow with heat transfer is one of the most applicable cases in various fields of engineering due to its industrial applications. The problem of a viscous fluid between two nonparallel walls meeting at a vertex and with a source of sink at the vertex was pioneered by Jeffery [1], and Hamel [2].

*Corresponding author.

Email addresses: vmarinca@mec.upt.ro (Vasile Marinca), remus.ene@upt.ro (Remus-Daniel Ene)

Later, the Jeffery-Hamel problem have been studied by several researchers and discussed in many textbooks and articles. A stationary problem with a finite number of "outlets" to infinity in the form of infinite sectors is considered by Rivkind and Solonnikov [3]. The problem of steady viscous flow in a convergent
10 channel is analyzed analytically and numerically for small, moderately large and asymptotically large Reynolds numbers over entire range of allowed convergence angles by Akulenko et al. [4]. The MHD Jeffery-Hamel problem is solved by Makinde and Mhone [5] using a special type of Hermite-Padé approximation semi-numerical approach and by Esmaili et al. [6] by applying Adomian decom-
15 position method. The classical Jeffery-Hamel flow problem is solved by Ganji et al. [7] by means of the variational iteration method and homotopy perturbation method, and by Joneidi et al. [8], by differential transformation method, Homotopy Perturbation Method and Homotopy Analysis Method. The classical Jeffery-Hamel problem was extended in [9] to include the effects of external
20 magnetic field in conducted fluid. Optimal homotopy asymptotic method is applied by Marinca and Herişanu [10] and by Esmaeilpour and Ganji [11]. The effect of magnetic field and nanoparticle on the Jeffery-Hamel flow are studied in [12] and [13]. Numerical treatment using stochastic algorithms is used by Raja and Samar [14].

25 In general, the problems as Jeffery-Hamel flows and other fluid mechanics problems are inherently nonlinear. Excepting a limited number of these problems most do not have analytical solution. The aim of this paper is to propose an accurate approach to the MHD Jeffery-Hamel flow with heat transfer problem using an analytical technique, namely OHPM [15], [16], [17]. Our approach
30 does not require a small or large parameter in the governing equations, is based on the construction and determination of some auxiliary functions combined with a convenient way to optimally control the convergence of the solution.

2. Problem statement and governing equations

We consider a system of cylindrical coordinates with a steady flow of an

35 incompressible conducting viscous fluid from a source or sink at channel walls
 lying in planes, with angle 2α , taking into account the effect of electromagnetic
 induction, as shown in Fig. 1, and the heat transfer.

The continuity equation, the Navier-Stokes equations and energy equation
 40 in cylindrical coordinates, can be written as [18], [19], [20], [21]:

$$\frac{1}{r} \frac{\partial}{\partial r} (ru_r) + \frac{1}{r} \frac{\partial}{\partial r} (ru_\varphi) = 0 \quad (1)$$

$$u_r \frac{\partial u_r}{\partial r} + \frac{u_\varphi}{r} \frac{\partial u_r}{\partial \varphi} - \frac{u_\varphi^2}{r} = -\frac{1}{\rho} \frac{\partial P}{\partial r} + \nu \left[\frac{1}{r} \frac{\partial(r\varepsilon_{rr})}{\partial r} + \frac{1}{r} \frac{\partial\varepsilon_{r\varphi}}{\partial r} - \frac{\varepsilon_{r\varphi}}{r} - \frac{\sigma B_0^2}{\rho r^2} u_r \right] \quad (2)$$

$$u_r \frac{\partial u_\varphi}{\partial r} + \frac{u_\varphi}{r} \frac{\partial u_\varphi}{\partial \varphi} - \frac{u_\varphi u_r}{r} = -\frac{1}{\rho r} \frac{\partial P}{\partial \varphi} + \nu \left[\frac{1}{r^2} \frac{\partial(r\varepsilon_{r\varphi})}{\partial r} + \frac{1}{r} \frac{\partial\varepsilon_{\varphi\varphi}}{\partial \varphi} - \frac{\varepsilon_{r\varphi}}{r} - \frac{\sigma B_0^2}{\rho r^2} u_\varphi \right] \quad (3)$$

$$u_r \frac{\partial T}{\partial r} = \frac{k}{\rho c_p} (\nabla^2 T) + \frac{\nu}{c_p} \left[2 \left(\left(\frac{\partial u_r}{\partial r} \right)^2 + \left(\frac{u_r}{r} \right)^2 \right) + \left(\frac{1}{r} \frac{\partial u_r}{\partial r} \right)^2 \right] + \frac{\sigma B_0^2}{\rho r^2} u_r^2 \quad (4)$$

45 where ρ is the fluid density, P is the pressure, ν is the kinematic viscosity, T
 is the temperature, k is the thermal conductivity, c_p is the specific heat at constant
 pressure, σ is the electrical conductivity, B_0 is the induced magnetic field
 and the stress components are defined as

$$\varepsilon_{rr} = 2 \frac{\partial u_r}{\partial r} - \frac{2}{3} \text{div} \bar{u} \quad (5)$$

50

$$\varepsilon_{\varphi\varphi} = \frac{2}{r} \frac{\partial u_\varphi}{\partial \varphi} + \frac{2u_r}{r} - \frac{2}{3} \text{div} \bar{u} \quad (6)$$

$$\varepsilon_{r\varphi} = \frac{2}{r} \frac{\partial u_r}{\partial \varphi} + 2 \frac{\partial}{\partial r} \left(\frac{u_\varphi}{r} \right) \quad (7)$$

By considering the velocity field is only along radial direction i.e. $u_\varphi = 0$ and
 substituting Eqs. (5)-(7) into Eqs. (2) and (3), the continuity, Navier-Stokes
 and energy equations become:

55

$$\frac{1}{r} \frac{\partial}{\partial r} (ru_r) = 0 \quad (8)$$

$$u_r \frac{\partial u_r}{\partial r} = -\frac{1}{\rho} \frac{\partial P}{\partial r} + \nu \left(\nabla^2 u_r - \frac{u_r}{r^2} - \frac{\sigma B^2}{\rho r^2} u_r \right) \quad (9)$$

$$-\frac{1}{\rho r} \frac{\partial P}{\partial \varphi} + \frac{2\nu}{r^2} \frac{\partial u_r}{\partial \varphi} = 0 \quad (10)$$

The relevant boundary conditions, due to the symmetry assumption at the channel centerline are as follows:

$$\frac{\partial u_r}{\partial \varphi} = \frac{\partial T}{\partial \varphi} = 0, \quad u_r = \frac{u_c}{r} \quad \text{at } \varphi = 0 \quad (11)$$

60 and at the plates making body of channel:

$$u_r = 0, \quad T = \frac{T_c}{r^2} \quad \text{at } \varphi = \alpha \quad (12)$$

where u_c and T_c are the centerline rate of movement and the constant wall temperature, respectively.

From the continuity equation (8), one can get

$$ru_r = f(\varphi) \quad (13)$$

65 where $f(\varphi)$ is an arbitrary function of φ only.

By integrating Eq. (10) it holds that

$$P(r, \varphi) = \frac{2\rho\nu}{r^2} f(\varphi) + \rho g(r) \quad (14)$$

in which $g(r)$ is an arbitrary function of r only.

Now, defining the dimensionless parameters:

70

$$\eta = \frac{\varphi}{\alpha}, \quad F(\eta) = \frac{f(\varphi)}{u_c}, \quad \theta(\eta) = r^2 \frac{T}{T_c} \quad (15)$$

where T_c is the ambient temperature, and substituting these into Eqs. (4) and (9) and then eliminating the pressure term, one can put:

$$F''' + 2\alpha Re F F' + (4 - H)\alpha^2 F' = 0 \quad (16)$$

$$\theta'' + 2\alpha(2\alpha + RePrF)\theta + \beta Pr \left[(H + 4\alpha^2)F^2 + F'^2 \right] = 0 \quad (17)$$

75 subject to the boundary conditions

$$F(0) = 1, \quad F'(0) = 0, \quad F(1) = 0 \quad (18)$$

$$\theta(1) = 0, \quad \theta'(0) = 0 \quad (19)$$

where $Re = \frac{\alpha u_c}{\nu}$ is the Reynolds number, $H = \sqrt{\frac{\sigma B_0^2}{\rho \nu}}$ is the Hartmann number, $Pr = \frac{\nu c_p}{k\rho}$, $\beta = \frac{u_c}{c_p}$ and prime denotes derivative with respect to η .

80 3. Basic ideas of optimal homotopy perturbation method

To explain the ideas of the optimal homotopy perturbation method, consider the non-linear differential equation

$$L[u, u', u'', u''', \eta] + g(\eta) + N[u, u', u'', u''', \eta] = 0 \quad (20)$$

that is subject to the initial / boundary condition:

$$B\left(u, \frac{\partial u}{\partial \eta}\right) = 0, \quad \eta \in \Gamma \quad (21)$$

where L is a linear operator, g is a known function, N a nonlinear operator, B is a boundary operator and Γ is the boundary of the domain of interest [15], [16], [17]. We construct the homotopy [22]

$$\mathcal{H}(u, p) = L(u, u', u'', u''', \eta) + g(\eta) + pN(u, u', u'', u''', \eta) = 0 \quad (22)$$

for Eq. (20), where p is the homotopy parameter, $p \in [0, 1]$. From Eq. (22) one gets:

90

$$\begin{aligned} \mathcal{H}(u, 0) &= L(u, u', u'', u''', \eta) + g(\eta) = 0 \\ \mathcal{H}(u, 1) &= L(u, u', u'', u''', \eta) + g(\eta) + N(u, u', u'', u''', \eta) = 0 \end{aligned} \quad (23)$$

Assuming that the approximate analytical solution of the second-order can be expressed in the form

$$\bar{u}(\eta) = u_0 + pu_1 + p^2u_2 \quad (24)$$

and expanding the nonlinear operator N in series, with respect to the parameter p , we have:

$$\begin{aligned} N(\bar{u}, \bar{u}', \bar{u}'', \bar{u}''', \eta) &= N(u_0, u_0', u_0'', u_0''', \eta) + p[u_1 N_{\bar{u}}(u_0, u_0', u_0'', u_0''', \eta) + \\ &+ u_1' N_{\bar{u}'}(u_0, u_0', u_0'', u_0''', \eta) + u_1'' N_{\bar{u}''}(u_0, u_0', u_0'', u_0''', \eta) + \\ &+ u_1''' N_{\bar{u}'''}(u_0, u_0', u_0'', u_0''', \eta)] + p^2(u_2 N_{\bar{u}} + u_2' N_{\bar{u}'} + \dots) \end{aligned} \quad (25)$$

where $F_{\bar{u}} = \frac{\partial F}{\partial \bar{u}}$. By introducing a number of unknown auxiliary functions $H_i(\eta, C_k)$, $i = 0, 1, 2, \dots$ that depend on the variable η and some parameters C_k , $k = 1, 2, \dots, s$, we can construct a new homotopy:

100

$$\begin{aligned} \mathcal{H}(\bar{u}, p) &= L(\bar{u}, \bar{u}', \bar{u}'', \bar{u}''', \eta) + g(\eta) + pH_0(\eta, C_k)N(u_0, u_0', u_0'', u_0''', \eta) + \\ &p^2[H_1(\eta, C_k)u_1 N_{\bar{u}}(u_0) + H_2(\eta, C_k)u_1' N_{\bar{u}'}(u_0) + H_3(\eta, C_k)u_1'' N_{\bar{u}''}(u_0) + \\ &+ H_4(\eta, C_k)u_1''' N_{\bar{u}'''}(u_0)] + p^2[H_5(\eta, C_k)u_2 N_{\bar{u}}(u_0) + H_6(\eta, C_k)u_2' N_{\bar{u}'}(u_0) + \dots] \end{aligned} \quad (26)$$

Equating the coefficients of like powers of p , yields the linear equations:

$$L[u_0, u_0', u_0'', u_0''', \eta] + g(\eta) = 0, \quad B\left(u_0, \frac{\partial u_0}{\partial \eta}\right) = 0 \quad (27)$$

$$L(u_1) + H_0(\eta, C_k)N(u_0, u_0', u_0'', u_0''', \eta) = 0, \quad B\left(u_1, \frac{\partial u_1}{\partial \eta}\right) = 0 \quad (28)$$

$$\begin{aligned} L(u_2) + H_1(\eta, C_k)u_1 N_{\bar{u}}(u_0, u_0', u_0'', u_0''', \eta) + H_2(\eta, C_k)u_1' N_{\bar{u}'}(u_0) + \\ + H_3(\eta, C_k)u_1'' N_{\bar{u}''}(u_0) + H_4(\eta, C_k)u_1''' N_{\bar{u}'''}(u_0) = 0, \quad B\left(u_2, \frac{\partial u_2}{\partial \eta}\right) = 0 \end{aligned} \quad (29)$$

105

The functions $H_i(\eta, C_k)$, $i = 0, 1, 2, \dots$ are not unique and can be chosen such that the products $H_i \cdot u_j N_u$ and $u_j N_u$ are of the same form. In this way, a maximum of only two iterations are required to achieve accurate solutions.

The unknown parameters C_k , $k = 1, 2, \dots, s$ which appear in the functions $H_i(\eta, C_k)$ can be determined optimally by means of the least-square method, collocation method, the weighted residuals, the Galerkin method, and so on.

In this way the solution of Eq. (20) subject to the initial / boundary condition (21) can be readily determined. It follows that the basic ideas of our procedure are the construction of a new homotopy (26), the auxiliary functions H_i with parameters C_k that can be determined optimally leading to the conclusion that the convergence of the approximate solutions can be easily controlled.

4. Application of OHPM to the MHD Jeffery-Hamel flow and heat transfer problem

Let us present the approximate analytic expressions of $f(\eta)$ and $\theta(\eta)$ from Eqs. (16)-(19) by means of OHPM.

For Eqs. (16) and (18), the linear operator is chosen as $L(F) = F'''$, while the nonlinear operator is defined as $N(F) = 2\alpha FF' + (4 - H)\alpha^2 F'$, $g(\eta) = 0$. The initial approximation F_0 is obtained from equation (27)

$$F_0''' = 0, \quad F_0(0) = 1, \quad F_0'(0) = 0, \quad F_0(1) = 0 \quad (30)$$

The solution of Eq. (30) is hence

$$F_0(\eta) = 1 - \eta^2. \quad (31)$$

On the other hand, from Eq. (16), one obtains

$$N_F(F) = 2\alpha Re F', \quad N_{F'}(F) = 2\alpha Re F + (4 - H)\alpha^2. \quad (32)$$

By substituting Eq. (31) into the nonlinear operator N and into Eq. (32) one retrieves:

$$\begin{aligned} N(F_0) &= 2A\eta^2 - 2(A + B)\eta, & N_F(F_0) &= -2A\eta, \\ N_{F'}(F_0) &= -A\eta^2 + A + B \end{aligned} \quad (33)$$

where $A = 2\alpha Re$, $B = (4 - H)\alpha^2$.

130 Eq. (28) becomes

$$F_1'''' + H_0(\eta, C_k) [2A\eta^2 - 2(A + B)\eta] = 0, \quad F_1(0) = F_1'(0) = F_1(1) = 0 \quad (34)$$

We choose $H_0(\eta, C_k) = -60C_1$ where C_1 is an unknown parameter and from Eq. (34) we obtain

$$F_1(\eta) = 2AC_1\eta^5 - 5(A + B)C_1\eta^4 + (3A + 5B)C_1\eta^2 \quad (35)$$

Eq. (29) can be written in the form

$$\begin{aligned} F_2'''' + H_1(\eta, C_k)(-2A\eta)F_1 + H_2(\eta, C_k)(-A\eta^2 + A + B)F_1' &= 0 \\ F_2(0) = F_2'(0) = F_2(1) &= 0 \end{aligned} \quad (36)$$

In this case we choose

$$H_1(\eta, C_k) = \frac{1}{2A} \left(C_2\eta^2 + C_3\eta + C_4 + \frac{C_5}{\eta} \right), \quad H_2(\eta, C_k) = \frac{C_6}{2} + \frac{C_7}{\eta}$$

135 such that the solution of Eq. (36) is given by

$$\begin{aligned} F_2(\eta) &= \frac{AC_1C_2}{495}\eta^{11} + \frac{2AC_1C_3-5(A+B)C_1C_2}{720}\eta^{10} + \\ &+ \frac{2AC_1C_4-5(A+B)C_1C_3+5A^2C_1C_6}{504}\eta^9 + \\ &+ \frac{(3A+5B)C_1C_2-5(A+B)C_1C_4+2AC_1C_5-10(A^2+AB)C_1C_6}{336}\eta^8 + \\ &+ \frac{(3A+5B)C_1C_3-5(A+B)C_1C_5-5(A^2+AB)C_1C_6+2AC_1C_7}{210}\eta^7 + \\ &+ \frac{(3A+5B)C_1C_4+(13A^2+25AB+10B^2)C_1C_6-5(A+B)C_1C_7}{120}\eta^6 + \\ &+ \frac{(3A+5B)C_1C_5}{60}\eta^5 - \frac{(3A^2+8AB+5B^2)C_1C_6+(3A+5B)C_1C_7}{24}\eta^4 + M\eta^2 \end{aligned} \quad (37)$$

where

$$\begin{aligned} M &= -C_1C_2 \left[\left(\frac{1}{495} - \frac{1}{144} + \frac{1}{112} \right) A + \left(\frac{5}{336} - \frac{1}{144} \right) B \right] - \\ &- C_1C_3 \left[\left(\frac{1}{360} - \frac{5}{504} + \frac{1}{70} \right) A + \left(\frac{1}{42} - \frac{5}{504} \right) B \right] - \\ &- C_1C_4 \left[\left(\frac{1}{252} - \frac{5}{336} + \frac{1}{40} \right) A + \left(\frac{1}{24} - \frac{5}{336} \right) B \right] - C_1C_5 \left(\frac{9A}{280} + \frac{5B}{84} \right) - \\ &- C_1C_6 \left[\left(\frac{5}{504} - \frac{5}{168} - \frac{5}{210} - \frac{1}{60} \right) A^2 - \left(\frac{5}{168} + \frac{5}{210} + \frac{1}{8} \right) AB - \frac{1}{8} B^2 \right] - C_1C_7 \left(\frac{13A}{140} + \frac{B}{6} \right) \end{aligned}$$

For $p = 1$ into Eq. (24), we obtain the second-order approximate solution, using and Eqs. (31), (35) and (37):

140

$$\begin{aligned}
\bar{F}(\eta) = & F_0(\eta) + F_1(\eta) + F_2(\eta) = \frac{AC_1C_2}{495}\eta^{11} + \frac{2AC_1C_3-5(A+B)C_1C_2}{720}\eta^{10} + \\
& + \frac{2AC_1C_4-5(A+B)C_1C_3+5A^2C_1C_6}{504}\eta^9 + \\
& + \frac{(3A+5B)C_1C_2-5(A+B)C_1C_4+2AC_1C_5-10(A^2+AB)C_1C_6}{336}\eta^8 + \\
& + \frac{(3A+5B)C_1C_3-5(A+B)C_1C_5-5(A^2+AB)C_1C_6+2AC_1C_7}{210}\eta^7 + \\
& + \frac{(3A+5B)C_1C_4+(13A^2+25AB+10B^2)C_1C_6-5(A+B)C_1C_7}{120}\eta^6 + \left(2AC_1 + \frac{(3A+5B)}{60}C_1C_5\right)\eta^5 - \\
& - \left[\frac{(3A^2+8AB+5B^2)C_1C_6+(3A+5B)C_1C_7}{24} + (5A + 5B)C_1\right]\eta^4 + [(3A + 5B) + M - 1]\eta^2
\end{aligned} \tag{38}$$

Now, we present the approximate analytic solution for Eqs. (17) and (19).

The linear and nonlinear operators and the function g are, respectively

$$\begin{aligned}
L(\theta) = & \theta'', \quad g(\eta) = -1, \\
N(\theta) = & 1 + 4\alpha^2\theta + 2\alpha RePrF\theta + \beta Pr \left[(1 + 4\alpha^2)F^2 + F'^2 \right]
\end{aligned} \tag{39}$$

The Eq. (27) becomes

$$\theta_0'' - 1 = 0, \quad \theta_0(1) = 0, \quad \theta_0'(0) = 0 \tag{40}$$

145

Eq. (40) has the solution

$$\theta_0(\eta) = \frac{1}{2}(1 - \eta^2). \tag{41}$$

From Eq. (39) it follows that

$$N_\theta(\theta) = 4\alpha^2 + 2\alpha RePrF, \quad N_{\theta'}(\theta) = 0. \tag{42}$$

By substituting Eq. (41) into Eqs. (39) and (42), one gets respectively

$$N(\theta_0) = C - 2D\eta^2 + E\eta^4, \quad N_\theta(\theta_0) = L + K\eta^2 \tag{43}$$

where

$$\begin{aligned}
C = & 1 + 2\alpha^2 + \alpha RePr + 4\beta\alpha^2 Pr + PrH\beta \\
D = & \alpha^2 + 2\alpha RePr + 2\beta Pr(2\alpha^2 - 1) + PrH\beta \\
E = & \alpha RePr + 4\beta\alpha^2 Pr + PrH\beta \\
L = & 4\alpha^2 + 2\alpha RePr, \quad K = -2\alpha RePr
\end{aligned} \tag{44}$$

Eq. (28) can put

$$\theta_1'' + h_0(\eta, C_8)(C - 2D\eta^2 + E\eta^4) = 0, \quad \theta_1(1) = \theta_1'(0) = 0. \quad (45)$$

Choosing $h_0(\eta, C_8) = -30C_8$ into Eq. (45), one obtains

$$\theta_1(\eta) = C_8 [15C(\eta^2 - 1) - 5D(\eta^4 - 1) + E(\eta^6 - 1)]. \quad (46)$$

Eq. (29) can be written in the form

$$\theta_2'' + h_1(\eta, C_k)(L + K\eta^2)\theta_1 = 0, \quad \theta_2(1) = \theta_2'(0) = 0 \quad (47)$$

and therefore it is natural to choose the auxiliary function h_1 as

$$h_1(\eta, C_k) = \frac{1}{C_8} (C_9 + C_{10}\eta + C_{11}\eta^2 + C_{12}\eta^3 + C_{13}\eta^4)$$

From Eq. (47), it can shown that

$$\begin{aligned} \theta_2(\eta) = & -L(15C - 5D + E) \left[\frac{1}{2}C_9(\eta^2 - 1) + \frac{1}{6}C_{10}(\eta^3 - 1) \right] + \\ & + [15LCC_9 - (15C - 5D + E)(KC_9 + LC_{11})] \frac{\eta^4 - 1}{12} + \\ & + [15LCC_{10} - (15C - 5D + E)(KC_{10} + LC_{12})] \frac{\eta^5 - 1}{20} + \\ & + [(15CK - 5DK)C_9 + 15LCC_{11} - \\ & - (15C - 5D + E)(KC_{11} + LC_{13})] \frac{\eta^6 - 1}{30} + \\ & + [(15CK - 5DL)C_{10} + 15LCC_{12} - K(15C - 5D + E)C_{12}] \frac{\eta^7 - 1}{42} + \\ & + [(LE - 5DK)C_9 + (15CK - 5DL)C_{11} + 15LCC_{13} - \\ & - K(15C - 5D + E)C_{13}] \frac{\eta^8 - 1}{56} + \\ & + [(LE - 5DK)C_{10} + (15CK - 5DL)C_{12}] \frac{\eta^9 - 1}{72} + \\ & + [EKC_9 + (LE - 5DK)C_{11} + (15CK - 5DL)C_{13}] \frac{\eta^{10} - 1}{90} + \\ & + [EKC_{11} + (LE - 5DK)C_{13}] \frac{\eta^{12} - 1}{132} + EKC_{12} \frac{\eta^{13} - 1}{156} + EKC_{13} \frac{\eta^{14} - 1}{182} \end{aligned} \quad (48)$$

The second-order approximate solution of Eqs. (17) and (19) is

$$\bar{\theta}(\eta) = \theta_0(\eta) + \theta_1(\eta) + \theta_2(\eta) \quad (49)$$

where θ_0 , θ_1 and θ_2 are given by Eqs. (41), (46) and (48) respectively.

5. Numerical results

160 In order to show the efficiency and accuracy of the OHPM , we consider some cases for different values of the parameters α and H . In all cases we consider $Re = 50, Pr = 1, \beta = 3.492161428 \cdot 10^{-13}$.

Case 5.1 Consider $\alpha = \frac{\pi}{24}$ and $H = 0$. By means of the least-square method, the values of the parameters $C_i, i = 1, 2, \dots, 13$ are

$$\begin{aligned} C_1 &= -0.000025737857, C_2 = 128165.4247848388, C_3 = -360860.8730122449, \\ C_4 &= 315974.73981422884, C_5 = -20823.768289134576, \\ C_6 &= -319.2089575339067, C_7 = -62701.61063351235, \\ C_8 &= -8.904447449602 \cdot 10^{-12}, C_9 = -2.9799239131772537 \cdot 10^{-12}, \\ C_{10} &= 0.441808726864 \cdot 10^{-12}, C_{11} = -1.808778662628 \cdot 10^{-12}, \\ C_{12} &= 0.111699001609 \cdot 10^{-12}, C_{13} = -5.293450955214 \cdot 10^{-12} \end{aligned}$$

One get approximate solutions from Eqs. (38) and (49) respectively:

$$\begin{aligned} \bar{F}(\eta) &= 1 - 2.3104494668\eta^2 + 2.4868857696\eta^4 + 0.3531718162\eta^5 - \\ &- 3.4153413394\eta^6 + 1.7515474936\eta^7 + 1.2031805064\eta^8 - \\ &- 1.6209066880\eta^9 + 0.6391440832\eta^{10} - 0.0872321749\eta^{11} \end{aligned} \quad (50)$$

165

$$\begin{aligned} \bar{\theta}(\eta) &= [-59.560673288998(\eta^2 - 1) - 9.116379402803(\eta^3 - 1) - \\ &- 142.753455187914(\eta^4 - 1) + 44.843714524611(\eta^5 - 1) + \\ &+ 168.833421156648(\eta^6 - 1) - 18.843109698135(\eta^7 - 1) - \\ &- 183.399486372212(\eta^8 - 1) + 2.145923952284(\eta^9 - 1) + \\ &+ 122.114218185962(\eta^{10} - 1) - 36.681425691368(\eta^{12} - 1) - \\ &- 0.061343981363(\eta^{13} - 1) + 2.491809125293(\eta^{14} - 1)] \cdot 10^{-12} \end{aligned} \quad (51)$$

Case 5.2 For $\alpha = \frac{\pi}{24}, H = 250$, the parameters C_i are:

$$C_1 = -0.011565849071, C_2 = 0.707159448177, C_3 = -290.324617452708,$$

$$\begin{aligned}
C_4 &= 435.512207098156, \quad C_5 = -98.780455208880, \\
C_6 &= -0.371954495218, \quad C_7 = -82.314218258861, \\
C_8 &= -37.285501459040 \cdot 10^{-12}, \quad C_9 = -15.253404678160 \cdot 10^{-12}, \\
C_{10} &= 12.572809436948 \cdot 10^{-12}, \quad C_{11} = -22.083271773195 \cdot 10^{-12}, \\
C_{12} &= 1.090339198400 \cdot 10^{-12}, \quad C_{13} = 14.241169061094 \cdot 10^{-12}
\end{aligned}$$

and therefore the approximate solutions, (38) and (49) may be written as:

$$\begin{aligned}
\bar{F}(\eta) &= 1 - 1.638305627622\eta^2 + 1.206009669620\eta^4 + 0.043648374556\eta^5 - \\
&- 1.078984595104\eta^6 + 0.156296141929\eta^7 + 0.738925954400\eta^8 - \\
&- 0.549972600570\eta^9 + 0.122598968736\eta^{10} - 0.000216285946\eta^{11}
\end{aligned} \tag{52}$$

$$\begin{aligned}
\bar{\theta}(\eta) &= [-1249.857282929460(\eta^2 - 1) - 9.116379418809(\eta^3 - 1) - \\
&- 956.378989402938(\eta^4 - 1) + 1351.297888810558(\eta^5 - 1) - \\
&- 1018.834483075130(\eta^6 - 1) - 646.214253910126(\eta^7 - 1) + \\
&+ 1232.314945834321(\eta^8 - 1) + 129.244515099455(\eta^9 - 1) - \\
&- 589.041009734213(\eta^{10} - 1) + 116.176788092689(\eta^{12} - 1) - \\
&- 0.598803450274(\eta^{13} - 1) - 6.703807283538(\eta^{14} - 1)] \cdot 10^{-12}
\end{aligned} \tag{53}$$

Case 5.3 For $\alpha = \frac{\pi}{24}$, $H = 500$ we obtain:

170

$$\begin{aligned}
\bar{F}(\eta) &= 1 - 1.1724778890\eta^2 + 0.4686048815\eta^4 - 0.098961423266\eta^5 - \\
&- 0.3550702077\eta^6 + 0.788918793543\eta^7 - 1.8412450049\eta^8 + \\
&+ 2.166714191416\eta^9 - 1.2119558765\eta^{10} + 0.255472535060\eta^{11}
\end{aligned} \tag{54}$$

$$\begin{aligned}
\bar{\theta}(\eta) &= [-3025.399926380127(\eta^2 - 1) - 9.116379434815(\eta^3 - 1) - \\
&- 3566.696711595512(\eta^4 - 1) + 4417.102370290691(\eta^5 - 1) - \\
&- 2124.393833887592(\eta^6 - 1) - 2172.379321553169(\eta^7 - 1) + \\
&+ 2808.629798261231(\eta^8 - 1) + 471.928890384626(\eta^9 - 1) - \\
&- 1267.595946519067(\eta^{10} - 1) + 212.551207395542(\eta^{12} - 1) - \\
&- 1.000321320275(\eta^{13} - 1) - 11.126037049812(\eta^{14} - 1)] \cdot 10^{-12}
\end{aligned} \tag{55}$$

Case 5.4 For $\alpha = \frac{\pi}{24}$, $H = 1000$, it holds that:

$$\begin{aligned} \bar{F}(\eta) = & 1 - 0.6223664982\eta^2 - 0.1660109481\eta^4 - 0.2259232591\eta^5 + \\ & + 0.415889430872\eta^6 - 0.5758423027\eta^7 + 0.198748794050\eta^8 + \\ & + 0.0038449003\eta^9 + 0.029311285675\eta^{10} - 0.0576514026\eta^{11} \end{aligned} \quad (56)$$

$$\begin{aligned} \bar{\theta}(\eta) = & [-8164.566371333924(\eta^2 - 1) - 9.116379466826(\eta^3 - 1) - \\ & - 12276.720695370957(\eta^4 - 1) + 13537.207073598438(\eta^5 - 1) - \\ & - 5217.969886112186(\eta^6 - 1) - 6768.312414390118(\eta^7 - 1) + \\ & + 8081.157802168993(\eta^8 - 1) + 1537.402367705613(\eta^9 - 1) - \\ & - 3743.086450834657(\eta^{10} - 1) + 613.584536626787(\eta^{12} - 1) - \\ & - 1.303403201992(\eta^{13} - 1) - 31.505440255694(\eta^{14} - 1)] \cdot 10^{-12} \end{aligned} \quad (57)$$

175

Case 5.5 For $\alpha = \frac{\pi}{36}$, $H = 0$, we obtain

$$\begin{aligned} \bar{F}(\eta) = & 1 - 1.7695466647\eta^2 + 1.2754140854\eta^4 + 0.1103023597\eta^5 - \\ & - 1.1550256736\eta^6 + 0.4434051824\eta^7 + 0.3358564399\eta^8 - \\ & - 0.3325192185\eta^9 + 0.1045556849\eta^{10} - 0.0124421957\eta^{11} \end{aligned} \quad (58)$$

$$\begin{aligned} \bar{\theta}(\eta) = & [-111.208165621670(\eta^2 - 1) - 6.895054111348(\eta^3 - 1) - \\ & - 219.101666428999(\eta^4 - 1) + 112.000412353392(\eta^5 - 1) + \\ & + 120.895605108821(\eta^6 - 1) - 47.637714830801(\eta^7 - 1) - \\ & - 104.355375516421(\eta^8 - 1) + 6.984672282609(\eta^9 - 1) + \\ & + 75.737792150272(\eta^{10} - 1) - 24.982664253556(\eta^{12} - 1) - \\ & - 0.097447216002(\eta^{13} - 1) + 1.768576986049(\eta^{14} - 1)] \cdot 10^{-12} \end{aligned} \quad (59)$$

Case 5.6 If $\alpha = \frac{\pi}{36}$, $H = 250$ then

$$\begin{aligned} \bar{F}(\eta) = & 1 - 1.5111014276\eta^2 + 0.8612876996\eta^4 + 0.0128407190\eta^5 - \\ & - 0.5668759509\eta^6 + 0.0367598458\eta^7 + 0.3198667899\eta^8 - \\ & - 0.1656253347\eta^9 + 0.0019977968\eta^{10} + 0.0108498620\eta^{11} \end{aligned} \quad (60)$$

$$\begin{aligned}
\bar{\theta}(\eta) = & [-5094.867741624686(\eta^2 - 1) - 6.895054147361(\eta^3 - 1) - \\
& -4500.773385702808(\eta^4 - 1) + 6249.12145418685(\eta^5 - 1) - \\
& -4283.444052831423(\eta^6 - 1) - 2834.31757828637(\eta^7 - 1) + \\
& +5102.615992457279(\eta^8 - 1) + 528.701361603855(\eta^9 - 1) - \\
& -2382.96513866767(\eta^{10} - 1) + 460.279590044557(\eta^{12} - 1) - \\
& -2.850139405026(\eta^{13} - 1) - 26.598784857626(\eta^{14} - 1)] \cdot 10^{-12}
\end{aligned} \tag{61}$$

Case 5.7 For $\alpha = \frac{\pi}{36}$, $H = 500$ the approximate solutions are

$$\begin{aligned}
\bar{F}(\eta) = & 1 - 1.2942214724\eta^2 + 0.5334630869\eta^4 + 0.0019708504\eta^5 - \\
& -0.3330602404\eta^6 - 0.0197377497\eta^7 + 0.2108709627\eta^8 - \\
& -0.1151093836\eta^9 + 0.0147650020\eta^{10} + 0.0010589440\eta^{11}
\end{aligned} \tag{62}$$

$$\begin{aligned}
\bar{\theta}(\eta) = & [-10479.441564298402(\eta^2 - 1) - 6.895054183374(\eta^3 - 1) - \\
& -9629.602717192312(\eta^4 - 1) + 12532.057010176612(\eta^5 - 1) - \\
& -7708.77471180501(\eta^6 - 1) - 5687.792565325205(\eta^7 - 1) + \\
& +9313.682156269786(\eta^8 - 1) + 1063.274966246270(\eta^9 - 1) - \\
& -4206.734533154069(\eta^{10} - 1) + 761.164805945711(\eta^{12} - 1) - \\
& -5.659649234867(\eta^{13} - 1) - 42.382058179415(\eta^{14} - 1)] \cdot 10^{-12}
\end{aligned} \tag{63}$$

Case 5.8 If $\alpha = \frac{\pi}{36}$, $H = 1000$ then

$$\begin{aligned}
\bar{F}(\eta) = & 1 - 0.9581900583\eta^2 + 0.0913634769\eta^4 + 0.0030073285\eta^5 - \\
& -0.1611067985\eta^6 + 0.0668486226\eta^7 - 0.0696973759\eta^8 + \\
& +0.0454374262\eta^9 - 0.0111066789\eta^{10} - 0.0065559425\eta^{11}
\end{aligned} \tag{64}$$

$$\begin{aligned}
\bar{\theta}(\eta) = & [-22457.262743604428(\eta^2 - 1) - 6.895054255400(\eta^3 - 1) - \\
& 22247.17539598977(\eta^4 - 1) + 26605.166448464304(\eta^5 - 1) - \\
& -14220.534699997283(\eta^6 - 1) - 12131.493178637833(\eta^7 - 1) + \\
& +17921.197074275697(\eta^8 - 1) + 2301.819882082563(\eta^9 - 1) - \\
& -7836.564793794578(\eta^{10} - 1) + 1301.948445444968(\eta^{12} - 1) - \\
& -11.186604132870(\eta^{13} - 1) - 68.576887703688(\eta^{14} - 1)] \cdot 10^{-12}
\end{aligned} \tag{65}$$

From the Tables 1-16 it is obvious that the second-order approximate solutions obtained by OHPM are of a high accuracy in comparison with homotopy perturbation method and with numerical solution obtained by means of a fourth-order Runge-Kutta method in combination with the shooting method using Wolfram Mathematica 6.0 software.

In Figs 2 and 3 are presented the effect of the Hartmann number on the velocity profile for $Re = 50$ and $\alpha = \frac{\pi}{24}$ and $\alpha = \frac{\pi}{36}$ respectively. It is observe that velocity increases with increasing of the Hartmann number for any value of α . The same effect of Hartmann number on the thermal profile are presented in Figs 4 and 5 for $\alpha = \frac{\pi}{24}$ and $\alpha = \frac{\pi}{36}$ respectively. In this case, the temperature decreases with increasing of the Hartmann number in the both cases. The effect of the half angle α on the velocity profile is presented in Figs 6-9. With an increasing value of α , velocity decreases for $H = 0$ and $H = 250$, but increases for $H = 500$ and $H = 1000$. From the Figs 11-13, it is interesting to remark that the temperature increases whereas the half angle α increases. In all cases, the maximum of temperature occurs near the walls for $H = 0$ and precisely in wall for $H \neq 0$, while the minimum occurs near the channel axis.

6. Conclusions

In present paper, the Optimal Homotopy Perturbation Method (OHPM) is employed to propose a new analytic approximate solutions for MHD Jeffery-Hamel flow with heat transfer problem. Our procedure does not need restrictive hypotheses, is very rapid convergent after only two iterations and the convergence of the solutions is ensured in a rigorous way. The cornerstone of the validity and flexibility of our procedure is the choice of the linear operator and the optimal auxiliary functions which contribute to very accurate solutions. The parameters which are involved in the composition of the optimal auxiliary functions are optimally identified via various methods in a rigorous way. Our technique is very effective, explicit, easy to apply which proves that this method

is very efficient in practice.

Conflict of Interests

The authors declare that there is no conflict of interests regarding the publication of this paper.

220 References

- [1] G. B. Jeffery, *The two-dimensional steady motion of a viscous fluid*, Philosophical Magazine, 6(20), 1915, 455–465.
- [2] G. Hamel, *Spiralförmige bewegungen zäher flüssigkeiten*, Jahresbericht der Deutschen Mathematiker-Vereinigung, 25, 1916, 34–60.
- 225 [3] L. Rivkind, V. A. Solonnikov, *Jeffery-Hamel asymptotics for steady state Navier-Stokes flow in domains with sector-like outlets to infinity*, J. Math. Fluid Mech., 2, 2000, 324–352.
- [4] L. D. Akulenko, D. V. Georgevskii, S. A. Kumakshev, *Solutions of the Jeffery-Hamel problem regularly extendable in the Reynolds number*, Fluid
230 Dynamics, 39(1), 2004, 12–28.
- [5] O. D. Makinde, P. Y. Mhone, *Hermite-Padé approximation approach to MHD Jeffery-Hamel flows*, Applied Math. and Comput., 181, 2006, 966–972.
- [6] Q. Esmaili, A. Ramiar, E. Alizadeh, D. D. Ganji, *An approximation of
235 the analytical solution of the Jeffery-Hamel flow by decomposition method*, Phys. Lett., 372, 2008, 3434–3439.
- [7] Z. Z. Ganji, D. D. Ganji, M. Esmailpour, *Study of nonlinear Jeffery-Hamel flow by He’s semi-analytical methods and comparison with numerical results*, Computers and Math with Appl., 58, 2009, 2107–2116.

- 240 [8] A. A. Joneidi, G. Domairry, M. Babaelahi, *Three analytical methods applied to Jeffery-Hamel flow*, Commun. Nonlin. Sci. Numer. Simulat., 15, 2010, 3423–3434.
- [9] S. M. Moghimi, D. D. Ganji, H. Bararnia, M. Hosseini, M. Jalbal, *Homotopy perturbation method for nonlinear MHD Jeffery-Hamel problem*,
245 Computers and Math. with Appl., 61, 2011, 2213–2216.
- [10] V. Marinca, N. Herişanu, *An optimal homotopy asymptotic approach applied to nonlinear MHD Jeffery-Hamel flow*, Mathematical Problems in Engineering, 2011, Article ID 169056, 16 pages.
- [11] M. Esmailpour, D. D. Ganji, *Solution of the Jeffery-Hamel flow problem by optimal homotopy asymptotic method*,
250 Comput. and Math. Appl., 59, 2010, 3405–3411.
- [12] M. Sheikholeshami, D. D. Ganji, H. R. Ashorynejad, H. B. Rokni, *Analytical investigation of Jeffery-Hamel flow with high magnetic field and nanoparticle by Adomian decomposition method*, Appl. Math. and Mech.,
255 Engl. ed., 33(1), 2012, 25–36.
- [13] A. K. Rostami, M. R. Akbari, D. D. Ganji, S. Heydari, *Investigating Jeffery-Hamel flow with high-magnetic field and nanoparticles by HPM and AGM*, Central Eur. J. of Eng., 4(4), 2014, 357–370.
- [14] M. A. Z. Raja, R. Samar, *Numerical treatment of nonlinear MHD Jeffery-Hamel problems using stochastic algorithms*,
260 Computers & Fluids, 91, 2014, 111–115.
- [15] V. Marinca, N. Herişanu, *Nonlinear Dynamical Systems in Engineering - Some Approximate Approaches*, Springer Verlag, Heidelberg, 2011.
- [16] V. Marinca, N. Herişanu, *Nonlinear dynamic analysis of an electrical machine rotor-bearing system by the optimal homotopy perturbation method*,
265 Computers and Math. with Appl., 61, 2011, 2019–2024.

- [17] N. Herişanu, V. Marinca, *Optimal homotopy perturbation method for a non-conservative dynamical system of a rotating electrical machine*, Z. Naturforsch, 67a, 2012, 509–516.
- 270 [18] H. Schlichting, *Boundary-layer theory* Mc Graw-Hill Book Company, 1979.
- [19] F. M. Ali, R. Nazar, N. M. Arifin, I. Pop, *MHD stagnation-point flow and heat transfer towards a stretching sheet with induced magnetic field*, Appl. Math. Mech., 32, 2011, 409–418.
- [20] S. H. Choi, H.-E. Wilhelm, *Incompressible magnetohydrodynamic flow with*
275 *heat transfer between inclined walls*, Physics of Fluids, 22, 1979, 1073–1078.
- [21] M. Turkyilmazoglu, *Extending the traditional Jeffery-Hamel flow to stretchable convergent / divergent channels*, Computers & Fluids, 100, 2014, 196–203.
- [22] J. H. He, *A coupling method of homotopy technique and perturbation technique for nonlinear problems*, Int. J. Non-Linear Mech., 35, 2000, 37–43.
280

Table 1. Comparison between the HPM results [9], OHPM results (50) and numerical results for the velocity $F(\eta)$ for $\alpha = \frac{\pi}{24}$ and $H = 0$

η	F_{HPM} [9]	F_{numeric}	\bar{F}_{OHPM} , Eq. (50)	relative error = $ F_{\text{numeric}} - \bar{F}_{\text{OHPM}} $
0	1	1	1	0
0.1	0.9770711	0.9771426047	0.9771444959	$1.8 \cdot 10^{-6}$
0.2	0.9112020	0.9114792278	0.9114802054	$9.7 \cdot 10^{-7}$
0.3	0.8104115	0.8110052403	0.8110054657	$2.2 \cdot 10^{-7}$
0.4	0.6859230	0.6869148220	0.6869163034	$1.4 \cdot 10^{-6}$
0.5	0.5498427	0.5512883212	0.5512895302	$1.2 \cdot 10^{-6}$
0.6	0.4131698	0.4151088947	0.4151091740	$2.7 \cdot 10^{-7}$
0.7	0.2846024	0.2870546320	0.2870554998	$8.6 \cdot 10^{-7}$
0.8	0.1702791	0.1731221390	0.1731231521	$1.01 \cdot 10^{-6}$
0.9	0.0744232	0.0768715756	0.0768721058	$5.3 \cdot 10^{-7}$
1	0	0	0	0

Table 2. Comparison between OHPM results (51) and numerical results for the temperature $\theta(\eta)$ for $\alpha = \frac{\pi}{24}$ and $H = 0$

η	θ_{numeric}	$\bar{\theta}_{\text{OHPM}}$ from Eq. (51)	relative error = $ \theta_{\text{numeric}} - \bar{\theta}_{\text{OHPM}} $
0	$-9.134405103300 \cdot 10^{-12}$	$-9.134559900000 \cdot 10^{-12}$	$1.5 \cdot 10^{-16}$
0.1	$-8.553981690585 \cdot 10^{-12}$	$-8.561731325450 \cdot 10^{-12}$	$7.7 \cdot 10^{-15}$
0.2	$-7.029011445513 \cdot 10^{-12}$	$-7.029011445531 \cdot 10^{-12}$	$1.7 \cdot 10^{-23}$
0.3	$-4.968059593695 \cdot 10^{-12}$	$-4.959904647105 \cdot 10^{-12}$	$8.1 \cdot 10^{-15}$
0.4	$-2.830354806908 \cdot 10^{-12}$	$-2.830354806921 \cdot 10^{-12}$	$1.3 \cdot 10^{-23}$
0.5	$-1.003581673783 \cdot 10^{-12}$	$-1.015625108634 \cdot 10^{-12}$	$1.2 \cdot 10^{-14}$
0.6	$2.755715234490 \cdot 10^{-13}$	$2.755715234410 \cdot 10^{-13}$	$7.9 \cdot 10^{-24}$
0.7	$9.398183452650 \cdot 10^{-13}$	$9.682947296376 \cdot 10^{-13}$	$2.8 \cdot 10^{-14}$
0.8	$1.062337244632 \cdot 10^{-12}$	$1.062337244629 \cdot 10^{-12}$	$3.3 \cdot 10^{-24}$
0.9	$7.684282928672 \cdot 10^{-13}$	$6.524090716991 \cdot 10^{-13}$	$1.1 \cdot 10^{-13}$
1	0	0	0

Table 3. Comparison between the HPM results [9], OHPM results (52) and numerical results for the velocity $F(\eta)$ for $\alpha = \frac{\pi}{24}$ and $H = 250$

η	F_{HPM} [9]	F_{numeric}	\bar{F}_{OHPM} , Eq. (52)	relative error = $ F_{\text{numeric}} - \bar{F}_{\text{OHPM}} $
0	1	1	1	0
0.1	0.9837340	0.9837367791	0.9837369246	$1.4 \cdot 10^{-7}$
0.2	0.9363350	0.9363459948	0.9363459260	$6.8 \cdot 10^{-8}$
0.3	0.8616894	0.8617133581	0.8617132189	$1.3 \cdot 10^{-7}$
0.4	0.7653405	0.7653814753	0.7653813980	$7.7 \cdot 10^{-8}$
0.5	0.6533961	0.6534573087	0.6534570226	$2.8 \cdot 10^{-7}$
0.6	0.5314621	0.5315466609	0.5315462975	$3.6 \cdot 10^{-7}$
0.7	0.4038130	0.4039227354	0.4039224205	$3.1 \cdot 10^{-7}$
0.8	0.2728708	0.2729980317	0.2729975130	$5.1 \cdot 10^{-7}$
0.9	0.1389433	0.1390416079	0.1390411070	$5.0 \cdot 10^{-7}$
1	0	0	0	0

Table 4. Comparison between OHPM results (53) and numerical results for the temperature $\theta(\eta)$ for $\alpha = \frac{\pi}{24}$ and $H = 250$

η	θ_{numeric}	$\bar{\theta}_{\text{OHPM}}$ from Eq. (53)	relative error = $ \theta_{\text{numeric}} - \bar{\theta}_{\text{OHPM}} $
0	$-8.520036945014 \cdot 10^{-10}$	$-8.520036944914 \cdot 10^{-10}$	$9.9 \cdot 10^{-21}$
0.1	$-8.394493067234 \cdot 10^{-10}$	$-8.395974340239 \cdot 10^{-10}$	$1.4 \cdot 10^{-13}$
0.2	$-8.032504411694 \cdot 10^{-10}$	$-8.032504411616 \cdot 10^{-10}$	$7.8 \cdot 10^{-21}$
0.3	$-7.450795118612 \cdot 10^{-10}$	$-7.450297754118 \cdot 10^{-10}$	$4.9 \cdot 10^{-14}$
0.4	$-6.677062404515 \cdot 10^{-10}$	$-6.677062404494 \cdot 10^{-10}$	$2.1 \cdot 10^{-21}$
0.5	$-5.746573136109 \cdot 10^{-10}$	$-5.746735798562 \cdot 10^{-10}$	$1.6 \cdot 10^{-14}$
0.6	$-4.698328124476 \cdot 10^{-10}$	$-4.698328124489 \cdot 10^{-10}$	$1.3 \cdot 10^{-21}$
0.7	$-3.570882806332 \cdot 10^{-10}$	$-3.571240799348 \cdot 10^{-10}$	$3.5 \cdot 10^{-14}$
0.8	$-2.398013591946 \cdot 10^{-10}$	$-2.398013591937 \cdot 10^{-10}$	$9.8 \cdot 10^{-22}$
0.9	$-1.206024561793 \cdot 10^{-10}$	$-1.200670094842 \cdot 10^{-10}$	$5.3 \cdot 10^{-13}$
1	0	0	0

Table 5. Comparison between the HPM results [9], OHPM results (54) and numerical results for the velocity $F(\eta)$ for $\alpha = \frac{\pi}{24}$ and $H = 500$

η	F_{HPM} [9]	F_{numeric}	\bar{F}_{OHPM} , Eq. (54)	relative error = $ F_{\text{numeric}} - \bar{F}_{\text{OHPM}} $
0	1	1	1	0
0.1	0.9883197	0.9883196668	0.9883207994	$1.1 \cdot 10^{-6}$
0.2	0.9537955	0.9537952479	0.9538026351	$7.3 \cdot 10^{-6}$
0.3	0.8978515	0.8978510438	0.8978610430	$9.9 \cdot 10^{-6}$
0.4	0.8224699	0.8224690439	0.8224696000	$5.5 \cdot 10^{-7}$
0.5	0.7296817	0.7296803425	0.7296719365	$8.4 \cdot 10^{-6}$
0.6	0.6209748	0.6209728597	0.6209706881	$2.1 \cdot 10^{-6}$
0.7	0.4966644	0.4966617866	0.4966700156	$8.2 \cdot 10^{-6}$
0.8	0.3552115	0.3552079113	0.3552097261	$1.8 \cdot 10^{-6}$
0.9	0.1923821	0.1923775215	0.1923683642	$9.1 \cdot 10^{-6}$
1	0	0	0	0

Table 6. Comparison between OHPM results (55) and numerical results for the temperature $\theta(\eta)$ for $\alpha = \frac{\pi}{24}$ and $H = 500$

η	θ_{numeric}	$\bar{\theta}_{\text{OHPM}}$ from Eq. (55)	relative error = $ \theta_{\text{numeric}} - \bar{\theta}_{\text{OHPM}} $
0	$-1.783303641361 \cdot 10^{-9}$	$-1.783303641351 \cdot 10^{-9}$	$9.9 \cdot 10^{-21}$
0.1	$-1.753016328789 \cdot 10^{-9}$	$-1.753373570315 \cdot 10^{-9}$	$3.5 \cdot 10^{-13}$
0.2	$-1.666810282194 \cdot 10^{-9}$	$-1.666810282186 \cdot 10^{-9}$	$7.8 \cdot 10^{-21}$
0.3	$-1.531366088677 \cdot 10^{-9}$	$-1.531258066872 \cdot 10^{-9}$	$1.08 \cdot 10^{-13}$
0.4	$-1.356325163065 \cdot 10^{-9}$	$-1.356325163062 \cdot 10^{-9}$	$2.1 \cdot 10^{-21}$
0.5	$-1.152391353408 \cdot 10^{-9}$	$-1.152436518900 \cdot 10^{-9}$	$4.5 \cdot 10^{-14}$
0.6	$-9.301091200084 \cdot 10^{-10}$	$-9.301091200095 \cdot 10^{-10}$	$1.1 \cdot 10^{-21}$
0.7	$-6.989817680976 \cdot 10^{-10}$	$-6.987973346248 \cdot 10^{-10}$	$1.8 \cdot 10^{-13}$
0.8	$-4.652100850091 \cdot 10^{-10}$	$-4.652100850080 \cdot 10^{-10}$	$1.1 \cdot 10^{-21}$
0.9	$-2.319273360260 \cdot 10^{-10}$	$-2.321569863571 \cdot 10^{-10}$	$2.2 \cdot 10^{-13}$
1	0	0	0

Table 7. Comparison between the HPM results [9], OHPM results (56) and numerical results for the velocity $F(\eta)$ for $\alpha = \frac{\pi}{24}$ and $H = 1000$

η	F_{HPM} [9]	F_{numeric}	\bar{F}_{OHPM} , Eq. (56)	relative error = $ F_{\text{numeric}} - \bar{F}_{\text{OHPM}} $
0	1	1	1	0
0.1	0.9937607	0.9937611413	0.9937578349	$3.3 \cdot 10^{-6}$
0.2	0.9747886	0.9747905377	0.9747871858	$3.3 \cdot 10^{-6}$
0.3	0.9422794	0.9422838643	0.9422837661	$9.8 \cdot 10^{-8}$
0.4	0.8947431	0.8947513541	0.8947499642	$1.3 \cdot 10^{-6}$
0.5	0.8297471	0.8297605618	0.8297564399	$4.1 \cdot 10^{-6}$
0.6	0.7434756	0.7434959928	0.7434941281	$1.8 \cdot 10^{-6}$
0.7	0.6299866	0.6300164190	0.6300167936	$3.7 \cdot 10^{-7}$
0.8	0.4799338	0.4799757286	0.4799724842	$3.2 \cdot 10^{-6}$
0.9	0.2782789	0.2783297889	0.2783280591	$1.7 \cdot 10^{-6}$
1	0	0	0	0

Table 8. Comparison between OHPM results (57) and numerical results for the temperature $\theta(\eta)$ for $\alpha = \frac{\pi}{24}$ and $H = 1000$

η	θ_{numeric}	$\bar{\theta}_{\text{OHPM}}$ from Eq. (57)	relative error = $ \theta_{\text{numeric}} - \bar{\theta}_{\text{OHPM}} $
0	$-3.885903481818 \cdot 10^{-9}$	$-3.885903481801 \cdot 10^{-9}$	$1.7 \cdot 10^{-20}$
0.1	$-3.804390715058 \cdot 10^{-9}$	$-3.805365047292 \cdot 10^{-9}$	$9.7 \cdot 10^{-13}$
0.2	$-3.575104095175 \cdot 10^{-9}$	$-3.575104095175 \cdot 10^{-9}$	$5.7 \cdot 10^{-23}$
0.3	$-3.222962704714 \cdot 10^{-9}$	$-3.222630117770 \cdot 10^{-9}$	$3.3 \cdot 10^{-13}$
0.4	$-2.782964569511 \cdot 10^{-9}$	$-2.782964569511 \cdot 10^{-9}$	$4.4 \cdot 10^{-23}$
0.5	$-2.293213461698 \cdot 10^{-9}$	$-2.293504856351 \cdot 10^{-9}$	$2.9 \cdot 10^{-13}$
0.6	$-1.790055410191 \cdot 10^{-9}$	$-1.790055410191 \cdot 10^{-9}$	$3.5 \cdot 10^{-23}$
0.7	$-1.302936492610 \cdot 10^{-9}$	$-1.301687731203 \cdot 10^{-9}$	$1.2 \cdot 10^{-12}$
0.8	$-8.442618285524 \cdot 10^{-10}$	$-8.442618285525 \cdot 10^{-10}$	$1.4 \cdot 10^{-23}$
0.9	$-4.107432220830 \cdot 10^{-10}$	$-4.158108458702 \cdot 10^{-10}$	$5.06 \cdot 10^{-12}$
1	0	0	0

Table 9. Comparison between the OHPM results (58) and numerical results for the velocity $F(\eta)$ for $\alpha = \frac{\pi}{36}$ and $H = 0$

η	F_{numeric}	\bar{F}_{OHPM} , Eq. (58)	relative error = $ F_{\text{numeric}} - \bar{F}_{\text{OHPM}} $
0	1	1	0
0.1	0.9824312364	0.9824320701	$8.3 \cdot 10^{-7}$
0.2	0.9312259577	0.9312265466	$5.8 \cdot 10^{-7}$
0.3	0.8506106161	0.8506107339	$1.1 \cdot 10^{-7}$
0.4	0.7467908018	0.7467915008	$6.9 \cdot 10^{-7}$
0.5	0.6269481682	0.6269490072	$8.3 \cdot 10^{-7}$
0.6	0.4982344464	0.4982347463	$2.9 \cdot 10^{-7}$
0.7	0.3669663386	0.3669668037	$4.6 \cdot 10^{-7}$
0.8	0.2381237463	0.2381245686	$8.2 \cdot 10^{-7}$
0.9	0.1151519312	0.1151523953	$4.6 \cdot 10^{-7}$
1	0	0	0

Table 10. Comparison between OHPM results (59) and numerical results for the temperature $\theta(\eta)$ for $\alpha = \frac{\pi}{36}$ and $H = 0$

η	θ_{numeric}	$\bar{\theta}_{\text{OHPM}}$ from Eq. (59)	relative error = $ \theta_{\text{numeric}} - \bar{\theta}_{\text{OHPM}} $
0	$-2.552530215568 \cdot 10^{-11}$	$-2.552530214568 \cdot 10^{-11}$	$9.9 \cdot 10^{-21}$
0.1	$-2.442980325655 \cdot 10^{-11}$	$-2.444079060328 \cdot 10^{-11}$	$1.09 \cdot 10^{-14}$
0.2	$-2.143998685224 \cdot 10^{-11}$	$-2.143998685224 \cdot 10^{-11}$	$1.9 \cdot 10^{-25}$
0.3	$-1.714518106214 \cdot 10^{-11}$	$-1.713385692946 \cdot 10^{-11}$	$1.1 \cdot 10^{-14}$
0.4	$-1.227729149275 \cdot 10^{-11}$	$-1.227729149275 \cdot 10^{-11}$	$1.3 \cdot 10^{-25}$
0.5	$-7.579058130819 \cdot 10^{-12}$	$-7.588196380463 \cdot 10^{-12}$	$9.1 \cdot 10^{-15}$
0.6	$-3.636709774083 \cdot 10^{-12}$	$-3.636709774083 \cdot 10^{-12}$	$1.6 \cdot 10^{-25}$
0.7	$-8.316369531201 \cdot 10^{-13}$	$-8.099883012752 \cdot 10^{-13}$	$2.1 \cdot 10^{-14}$
0.8	$6.930669117891 \cdot 10^{-13}$	$6.930669117890 \cdot 10^{-13}$	$7.8 \cdot 10^{-26}$
0.9	$9.721365514984 \cdot 10^{-13}$	$8.898023093848 \cdot 10^{-13}$	$8.2 \cdot 10^{-14}$
1	0	0	0

Table 11. Comparison between the OHPM results (60) and numerical results for the velocity $F(\eta)$ for $\alpha = \frac{\pi}{36}$ and $H = 250$

η	F_{numeric}	\bar{F}_{OHPM} , Eq. (60)	relative error = $ F_{\text{numeric}} - \bar{F}_{\text{OHPM}} $
0	1	1	0
0.1	0.9849746347	0.9849746827	$4.8 \cdot 10^{-8}$
0.2	0.9409030596	0.9409030371	$2.2 \cdot 10^{-8}$
0.3	0.8706210985	0.8706210491	$4.9 \cdot 10^{-8}$
0.4	0.7783094304	0.7783094038	$2.6 \cdot 10^{-8}$
0.5	0.6688194854	0.6688193877	$9.7 \cdot 10^{-8}$
0.6	0.5469607278	0.5469605971	$1.3 \cdot 10^{-7}$
0.7	0.4168757453	0.4168756336	$1.1 \cdot 10^{-7}$
0.8	0.2815737222	0.2815735380	$1.8 \cdot 10^{-7}$
0.9	0.1426291045	0.1426289244	$1.8 \cdot 10^{-7}$
1	0	0	0

Table 12. Comparison between OHPM results (61) and numerical results for the temperature $\theta(\eta)$ for $\alpha = \frac{\pi}{36}$ and $H = 250$

η	θ_{numeric}	$\bar{\theta}_{\text{OHPM}}$ from Eq. (61)	relative error = $ \theta_{\text{numeric}} - \bar{\theta}_{\text{OHPM}} $
0	$-3.397742006028 \cdot 10^{-9}$	$-3.397742006018 \cdot 10^{-9}$	$9.9 \cdot 10^{-21}$
0.1	$-3.346638363267 \cdot 10^{-9}$	$-3.347192325339 \cdot 10^{-9}$	$5.5 \cdot 10^{-13}$
0.2	$-3.199501303768 \cdot 10^{-9}$	$-3.199501303768 \cdot 10^{-9}$	$1.9 \cdot 10^{-22}$
0.3	$-2.964278501171 \cdot 10^{-9}$	$-2.964072110215 \cdot 10^{-9}$	$2.06 \cdot 10^{-13}$
0.4	$-2.653181572584 \cdot 10^{-9}$	$-2.653181572584 \cdot 10^{-9}$	$6.7 \cdot 10^{-23}$
0.5	$-2.281170448213 \cdot 10^{-9}$	$-2.281224162207 \cdot 10^{-9}$	$5.3 \cdot 10^{-14}$
0.6	$-1.864037686164 \cdot 10^{-9}$	$-1.864037686164 \cdot 10^{-9}$	$1.4 \cdot 10^{-23}$
0.7	$-1.416766717489 \cdot 10^{-9}$	$-1.416988166987 \cdot 10^{-9}$	$2.2 \cdot 10^{-13}$
0.8	$-9.521674889800 \cdot 10^{-10}$	$-9.521674889800 \cdot 10^{-10}$	$2.8 \cdot 10^{-24}$
0.9	$-4.798620033623 \cdot 10^{-10}$	$-4.772452449206 \cdot 10^{-10}$	$2.6 \cdot 10^{-12}$
1	0	0	0

Table 13. Comparison between the OHPM results (62) and numerical results for the velocity $F(\eta)$ for $\alpha = \frac{\pi}{36}$ and $H = 500$

η	F_{numeric}	\bar{F}_{OHPM} , Eq. (62)	relative error = $ F_{\text{numeric}} - \bar{F}_{\text{OHPM}} $
0	1	1	0
0.1	0.9871108049	0.9871108182	$1.3 \cdot 10^{-8}$
0.2	0.9490642316	0.9490642266	$5.0 \cdot 10^{-9}$
0.3	0.8876104540	0.8876104486	$5.3 \cdot 10^{-9}$
0.4	0.8053144512	0.8053144616	$1.03 \cdot 10^{-8}$
0.5	0.7051032297	0.7051032241	$5.5 \cdot 10^{-9}$
0.6	0.5897534597	0.5897534552	$4.4 \cdot 10^{-9}$
0.7	0.4613867287	0.4613867398	$1.1 \cdot 10^{-8}$
0.8	0.3210064088	0.3210063961	$1.2 \cdot 10^{-8}$
0.9	0.1680649652	0.1680649814	$1.6 \cdot 10^{-8}$
1	0	0	0

Table 14. Comparison between OHPM results (63) and numerical results for the temperature $\theta(\eta)$ for $\alpha = \frac{\pi}{36}$ and $H = 500$

η	θ_{numeric}	$\bar{\theta}_{\text{OHPM}}$ from Eq. (63)	relative error = $ \theta_{\text{numeric}} - \bar{\theta}_{\text{OHPM}} $
0	$-6.861779213872 \cdot 10^{-9}$	$-6.861779213862 \cdot 10^{-9}$	$9.9 \cdot 10^{-21}$
0.1	$-6.756689795935 \cdot 10^{-9}$	$-6.757837516749 \cdot 10^{-9}$	$1.1 \cdot 10^{-12}$
0.2	$-6.454596023395 \cdot 10^{-9}$	$-6.454596023395 \cdot 10^{-9}$	$1.4 \cdot 10^{-23}$
0.3	$-5.973076729675 \cdot 10^{-9}$	$-5.972618579646 \cdot 10^{-9}$	$4.5 \cdot 10^{-13}$
0.4	$-5.338639377096 \cdot 10^{-9}$	$-5.338639377096 \cdot 10^{-9}$	$5.7 \cdot 10^{-24}$
0.5	$-4.583265280198 \cdot 10^{-9}$	$-4.583356882876 \cdot 10^{-9}$	$9.1 \cdot 10^{-14}$
0.6	$-3.739726496008 \cdot 10^{-9}$	$-3.739726496008 \cdot 10^{-9}$	$6.6 \cdot 10^{-24}$
0.7	$-2.838920429095 \cdot 10^{-9}$	$-2.839180849233 \cdot 10^{-9}$	$2.6 \cdot 10^{-13}$
0.8	$-1.906149341683 \cdot 10^{-9}$	$-1.906149341683 \cdot 10^{-9}$	$5.7 \cdot 10^{-24}$
0.9	$-9.597066242185 \cdot 10^{-10}$	$-9.553857275377 \cdot 10^{-10}$	$4.3 \cdot 10^{-12}$
1	0	0	0

Table 15. Comparison between the OHPM results (64) and numerical results for the velocity $F(\eta)$ for $\alpha = \frac{\pi}{36}$ and $H = 1000$

η	F_{numeric}	\bar{F}_{OHPM} , Eq. (64)	relative error = $ F_{\text{numeric}} - \bar{F}_{\text{OHPM}} $
0	1	1	0
0.1	0.9904272110	0.9904271107	$1.003 \cdot 10^{-7}$
0.2	0.9618100677	0.9618099299	$1.3 \cdot 10^{-7}$
0.3	0.9144036356	0.9144036639	$2.8 \cdot 10^{-8}$
0.4	0.8484736891	0.8484737167	$2.7 \cdot 10^{-8}$
0.5	0.7640642211	0.7640640849	$1.3 \cdot 10^{-7}$
0.6	0.6606772356	0.6606771839	$5.1 \cdot 10^{-8}$
0.7	0.5368520578	0.5368521821	$1.2 \cdot 10^{-7}$
0.8	0.3896018441	0.3896017829	$6.1 \cdot 10^{-8}$
0.9	0.2136111325	0.2136111294	$3.1 \cdot 10^{-9}$
1	0	0	0

Table 16. Comparison between OHPM results (65) and numerical results for the temperature $\theta(\eta)$ for $\alpha = \frac{\pi}{36}$ and $H = 1000$

η	θ_{numeric}	$\bar{\theta}_{\text{OHPM}}$ from Eq. (65)	relative error = $ \theta_{\text{numeric}} - \bar{\theta}_{\text{OHPM}} $
0	$-1.406496797937 \cdot 10^{-8}$	$-1.406496797936 \cdot 10^{-8}$	$9.9 \cdot 10^{-21}$
0.1	$-1.383991714524 \cdot 10^{-8}$	$-1.384237616580 \cdot 10^{-8}$	$2.4 \cdot 10^{-12}$
0.2	$-1.319483359510 \cdot 10^{-8}$	$-1.319483359510 \cdot 10^{-8}$	$8.2 \cdot 10^{-24}$
0.3	$-1.217244871718 \cdot 10^{-8}$	$-1.217139646331 \cdot 10^{-8}$	$1.05 \cdot 10^{-12}$
0.4	$-1.083591345359 \cdot 10^{-8}$	$-1.083591345359 \cdot 10^{-8}$	$1.1 \cdot 10^{-23}$
0.5	$-9.260353523538 \cdot 10^{-9}$	$-9.260364501045 \cdot 10^{-9}$	$1.09 \cdot 10^{-14}$
0.6	$-7.519751014022 \cdot 10^{-9}$	$-7.519751014022 \cdot 10^{-9}$	$4.9 \cdot 10^{-24}$
0.7	$-5.683228753360 \cdot 10^{-9}$	$-5.683311365697 \cdot 10^{-9}$	$8.2 \cdot 10^{-14}$
0.8	$-3.802282135607 \cdot 10^{-9}$	$-3.802282135607 \cdot 10^{-9}$	$3.3 \cdot 10^{-24}$
0.9	$-1.908111552553 \cdot 10^{-9}$	$-1.902733734257 \cdot 10^{-9}$	$5.3 \cdot 10^{-12}$
1	0	0	0

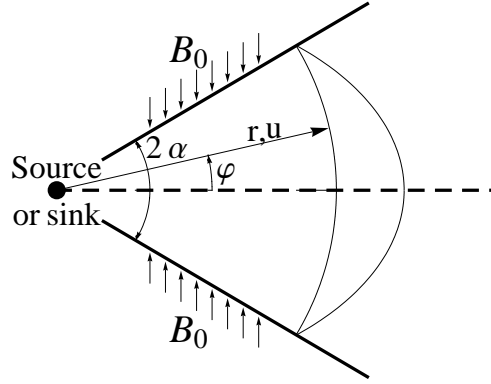


Fig 1. Geometry of the MHD Jeffery-Hamel problem.

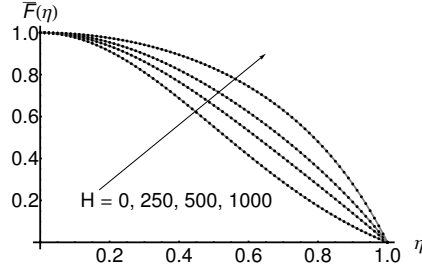


Fig. 2 Effect of the Hartmann number on the velocity profile for $\alpha = \pi/24, Re = 50$:
 — numerical solution,
 OHPM solution

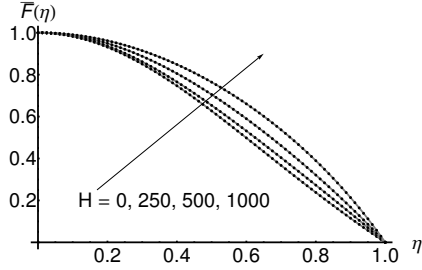


Fig. 3 Effect of the Hartmann number on the velocity profile for $\alpha = \pi/36, Re = 50$:
 — numerical solution,
 OHPM solution

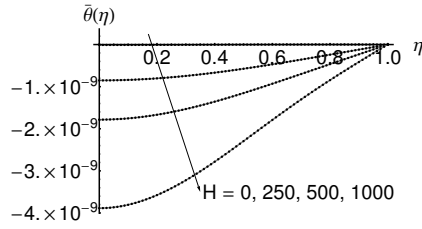


Fig. 4 Effect of the Hartmann number on the thermal profile for $\alpha = \pi/24, Re = 50$:
 — numerical solution,
 OHPM solution

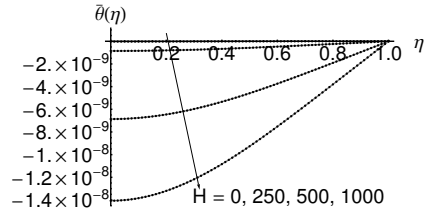


Fig. 5 Effect of the Hartmann number on the thermal profile for $\alpha = \pi/36, Re = 50$:
 — numerical solution,
 OHPM solution

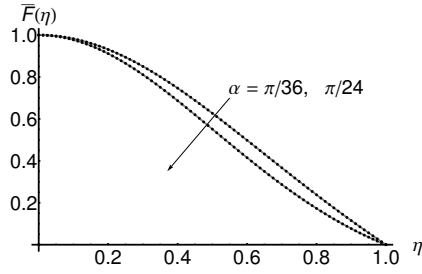


Fig. 6 Velocity profile for $\alpha = \pi/36$,
and $\alpha = \pi/24$, $H = 0$, $Re = 50$,

Eqs. (50) and (58):

— numerical solution,
..... OHPM solution

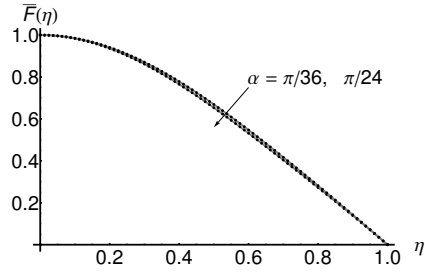


Fig. 7 Velocity profile for $\alpha = \pi/36$,
and $\alpha = \pi/24$, $H = 250$, $Re = 50$,

Eqs. (52) and (60):

— numerical solution,
..... OHPM solution

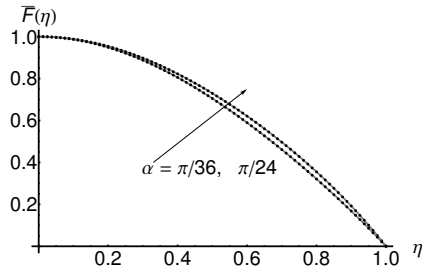


Fig. 8 Velocity profile for $\alpha = \pi/36$,
and $\alpha = \pi/24$, $H = 500$, $Re = 50$,

Eqs. (54) and (62):

— numerical solution,
..... OHPM solution

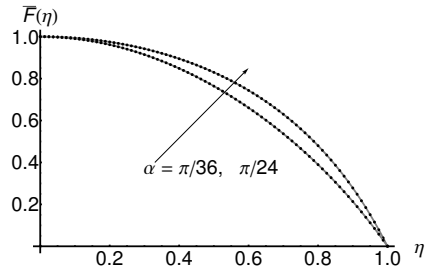


Fig. 9 Velocity profile for $\alpha = \pi/36$,
and $\alpha = \pi/24$, $H = 1000$, $Re = 50$,

Eqs. (56) and (64):

— numerical solution,
..... OHPM solution

285

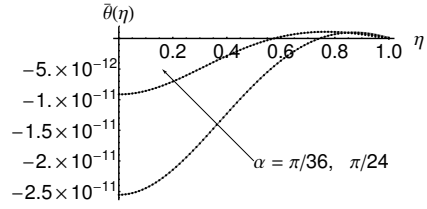


Fig. 10 Thermal profile for $\alpha = \pi/36$,
and $\alpha = \pi/24$, $H = 0$, $Re = 50$,
Eqs. (51) and (59):

— numerical solution,
..... OHPM solution

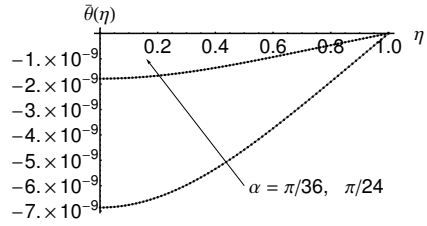


Fig. 12 Thermal profile for $\alpha = \pi/36$,
and $\alpha = \pi/24$, $H = 500$, $Re = 50$,
Eqs. (55) and (63):

— numerical solution,
..... OHPM solution

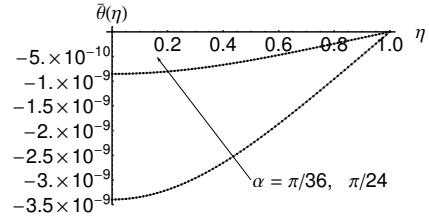


Fig. 11 Thermal profile for $\alpha = \pi/36$,
and $\alpha = \pi/24$, $H = 250$, $Re = 50$,
Eqs. (53) and (61):

— numerical solution,
..... OHPM solution

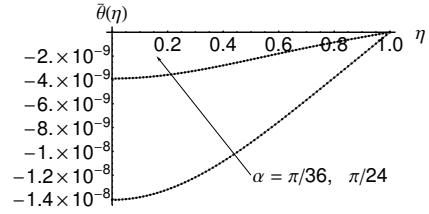


Fig. 13 Thermal profile for $\alpha = \pi/36$,
and $\alpha = \pi/24$, $H = 1000$, $Re = 50$,
Eqs. (57) and (65):

— numerical solution,
..... OHPM solution